# Model Order Reduction of Parametrized Nonlinear Reaction-Diffusion Systems

Martin A. Grepl[1]

*RWTH Aachen University, Numerical Mathematics, Templergraben 55, 52056 Aachen, Germany*

**Abstract**

We present a model order reduction technique for parametrized nonlinear reaction-diffusion systems. In our approach we combine the reduced basis method — a computational framework for rapid evaluation of functional outputs associated with the solution of parametrized partial differential equations — with the empirical interpolation method — a tool to construct "affine" coefficient-function approximations of nonlinear parameter dependent functions. We develop an efficient offline-online computational procedure for the evaluation of the reduced basis approximation: in the offline stage, we generate the reduced basis space; in the online stage, given a new parameter value, we calculate the reduced basis output. The operation count for the online stage depends only on the dimension of the reduced order model and the parametric complexity of the problem. The method is thus ideally suited for the many-query or real-time contexts. We present numerical results for a non-isothermal reaction-diffusion model to confirm and test our approach.

*Email address:* grepl@igpm.rwth-aachen.de (Martin A. Grepl)
[1]Tel.: +49 241 8096470, Fax: +49 241 80696470

*Keywords:* Reaction-Diffusion Equation, Model Order Reduction, Reduced Basis Approximation, Empirical Interpolation Method, Nonlinear Systems

## 1. Introduction

Nonlinear reaction-diffusion systems appear in a large number of real-world applications: ranging from Biology, to Ecology, to Physiology, to Chemistry (Smoller, 1994). Inherent to these equations and the specific application area are a large number of parameters – such as reaction rates or diffusion coefficients — which, in general, have a very strong influence on the dynamic behavior of the system. To analyze and understand the specific problem, many different parameter combinations have to be investigated. The solution of reaction-diffusion systems, however, is a very challenging task because the equations are time-dependent, often highly nonlinear, and coupled. Efficient solution techniques which can characterize many parameter combinations are therefore important. Furthermore, in many applications — such as chemical engineering — understanding, modeling, and simulation is often only the first step; the actual goal is the design, optimization, or real-time control of the problem of interest. Model order reduction techniques are vital in achieving these goals, see e.g. (Marquardt, 2002; Shvartsman et al., 2000; Christofides, 2001a,b) and (Shvartsman and Kevrekidis, 1998; Balsa-Canto et al., 2004).

In this paper we propose a model order reduction technique for nonlinear reaction-diffusion systems whose general formulation is given by

$$\frac{\partial \mathbf{y}(x,t;\mu)}{\partial t} = \nabla \left(\underline{D}(\mu)\nabla \mathbf{y}(x,t;\mu)\right) + \mathbf{g}(\mathbf{y}(x,t;\mu);\mu), \tag{1}$$

where $x \in \Omega \subset R^d$ is the spatial domain, $\mu \in \mathcal{D}$ is the parameter vector, $\mathbf{y}$ is the vector-valued field variable, e.g., containing temperatures and concentrations, $\underline{D}(\mu)$ is the diffusion matrix, and $\mathbf{g}(\mathbf{y};\mu)$ is a vector-valued function containing the (non)linear reaction terms. Our particular application is the self-ignition of a coal stockpile with Arrhenius type nonlinearity (Brooks et al., 1988). We note, however, that similar models are also used in combustion theory (Williams, 1985), biology (Britton, 1986), and in the description of porous catalysts (Aris, 1975a,b).

Many model-order reduction (MOR) techniques for linear and nonlinear time-dependent systems are proposed in the literature: the most well-known are proper orthogonal decomposition (POD or Karhunen-Loève decomposition) (Sirovich and Kirby, 1987; Sirovich, 1987; Holmes et al., 1996), balanced truncation (Moore, 1981), and various related hybrid (Lall et al., 1999, 2002; Hahn and Edgar, 2002; Willcox and Peraire, 2002; Rowley, 2005) techniques. It is important to note, however, that most MOR techniques focus mainly on reduced-order modeling of dynamical systems in which time is considered the *only* "parameter." The development of reduced-order models for problems with a simultaneous dependence of the field variable on parameter and time — our focus here — is much less common (see (Bui et al., 2003; Christensen et al., 2000; Daniel et al., 2002; Gunzburger et al., 2007) for a few exceptions). Furthermore, it is well known that most MOR techniques for nonlinear systems do not result in computational savings compared to the underlying high-dimensional model despite the often significant dimension reduction (Rathinam and Petzold, 2003). This is due to the fact that the computational cost to evaluate the nonlinearity in the reduced order model,

i.e., assembly and subsequent projection, still depends on the dimension of the original high-dimensional model. In most cases this cost outweighs the cost of solving the nonlinear system of equations. Two approaches to resolve this issue have been proposed previously in (Astrid, 2004) and (Romijn et al., 2008).

Our goal is the development of a model order reduction technique for coupled nonlinear reaction-diffusion systems that permits ($i$) the simultaneous dependence of the field variable (and output) on both time and parameters, and ($ii$) an efficient offline-online computational procedure which results in significant computational savings when solving the reduced system. To achieve these goals we pursue the reduced basis method (Prud'homme et al., 2002); see (Rozza et al., 2008) for a recent review of contributions to the methodology. The reduced basis method is a model order reduction technique that has proven to admit efficient and reliable reduced-order approximations for a large class of parametrized partial differential equations. For linear time-dependent problems we refer the interested reader to, e.g., (Grepl and Patera, 2005; Rovas et al., 2005; Haasdonk and Ohlberger, 2008), and for nonlinear problems to, e.g., (Veroy and Patera, 2005; Grepl et al., 2007; Nguyen and Peraire, 2008; Knezevic et al., 2011). More specifically, reduced basis approximation of reaction-diffusion systems were first considered in (Grepl, 2005).

This paper is organized as follows: In Section 2 we provide a review of the reduced basis method for parametrized nonlinear parabolic problems. In Section 3 we extend the methodology to treat nonlinear reaction-diffusion systems. As a specific example, we consider a model for the self-ignition of a

coal stockpile with Arrhenius type nonlinearity. Numerical results showing the performance of our model order reduction technique are presented in Section 4. We offer concluding remarks in Section 5.

## 2. Methodology

We present a review of the reduced basis method for scalar parametrized nonlinear parabolic problems. The presentation of this section is as follows: first, we introduce an abstract problem statement; we then introduce the empirical interpolation method for constructing a coefficient-function approximation of the nonlinear term; finally, we develop the reduced basis approximation for nonlinear parabolic problems and discuss computational complexity.

### *2.1. Problem Formulation*

Our focus here is on nonlinear parabolic partial differential equations (PDEs) with parametric dependence. The reduced basis approximation is based on the weak formulation of the governing equation. We therefore state the general abstract formulation and subsequently present a concrete example: a nonlinear reaction-diffusion equation with Arrhenius type nonlinearity.

For simplicity, we directly consider a time-discrete framework associated to the time interval $I \equiv ]0, t_f]$ ($\bar{I} \equiv [0, t_f]$). We divide $\bar{I}$ into $K$ subintervals of equal length $\Delta t = \frac{t_f}{K}$ and define $t^k \equiv k\Delta t$, $0 \leq k \leq K$; for notational convenience, we also introduce $\mathbb{K} \equiv \{1, \ldots, K\}$. We shall consider Euler-Backward for the time integration; we can also readily treat higher-order schemes such as Crank-Nicolson (Grepl, 2005).

The abstract formulation can be stated as follows: given a parameter $\mu \in \mathcal{D} \subset \mathbb{R}^P$, the field variable $y^{\mathrm{e}}(x, t^k; \mu) \in Y^{\mathrm{e}}$, $\forall k \in \mathbb{K}$, satisfies the weak form of the $\mu$-parametrized parabolic PDE

$$m(y^{\mathrm{e}}(t^k;\mu), v) + \Delta t\ a(y^{\mathrm{e}}(t^k;\mu), v; \mu) + \Delta t \int_\Omega g(y^{\mathrm{e}}(t^k;\mu); x; \mu)\, v \\ = m(y^{\mathrm{e}}(t^{k-1};\mu), v) + \Delta t\ f(v)\ u(t^k),\ \forall v \in Y^{\mathrm{e}},\ \forall k \in \mathbb{K}, \quad (2)$$

with initial condition (say) $y^{\mathrm{e}}(x, t^0; \mu) = 0$. Here, $\mathcal{D}$ is the parameter domain in which our $P$-tuple (input) parameter $\mu$ resides; $Y^{\mathrm{e}}$ is an appropriate Hilbert space; and $\Omega \subset \mathbb{R}^d$ is our spatial domain, a point in which shall be denoted $x$. Furthermore, $f(\cdot)$ and $a(\cdot, \cdot; \mu)$, $m(\cdot, \cdot)$ are continuous bounded linear and bilinear forms, respectively; $u(t^k)$ denotes the "control input" at time $t = t^k$; and $g(w; x; \mu)$ is a nonlinear function continuous in its arguments. We assume here that $f(\cdot)$, and $m(\cdot, \cdot)$ do not depend on the parameter; parameter dependence, however, is readily admitted (Grepl and Patera, 2005). We note that if an explicit scheme such as Euler-Forward is used, we then arrive at a linear system for $y^{\mathrm{e}}(t^k; \mu)$ but now burdened with a conditional stability restriction on $\Delta t$. In that case, the discrete reduced basis system will also be inheritedly linear.

In general, we are not interested in the field variable – such as temperature – at all points in $\Omega$ per se, but rather at specific performance metrics or outputs – such as averaged temperatures or heat fluxes – of the system. These outputs are typically functionals of the field variable: given the solution $y^{\mathrm{e}}(x, t^k; \mu) \in Y^{\mathrm{e}}$, $\forall k \in \mathbb{K}$, of (2), we evaluate the (here, single) output of interest from

$$s^{\mathrm{e}}(t^k; \mu) = \ell(y^{\mathrm{e}}(t^k; \mu)), \quad \forall k \in \mathbb{K}, \quad (3)$$

where $\ell(\cdot)$ is a linear bounded functional.

The superscript e denotes the "exact" — more precisely, semi-discrete — problem. In actual practice, of course, we do not have access to the exact solution; we thus replace the exact solution with a reference (or "truth") approximation, which resides in (say) a suitably fine piecewise-linear finite element approximation space $Y \subset Y^{\rm e}$ of *very* large dimension $\mathcal{N}$. We associated to $Y$ a set of piecewise linear (over each element) basis functions $\phi_i(x),\ 1 \le i \le \mathcal{N}$. Our "truth" finite element approximation $y^k(\mu) \equiv y(t^k;\mu) \in Y$ to the semi-discrete problem (2) is then given by

$$m(y^k(\mu),v) + \Delta t\ a(y^k(\mu),v;\mu) + \Delta t \int_\Omega g(y^k(\mu);x;\mu)\, v \\ = m(y^{k-1}(\mu),v) + \Delta t\ f(v)\ u(t^k),\ \forall v \in Y,\ \forall k \in \mathbb{K}, \quad (4)$$

with initial condition $y(t^0;\mu) = 0$; we then evaluate the output $s^k(\mu) \equiv s(t^k;\mu) \in \mathbb{R}$ from

$$s^k(\mu) = \ell(y^k(\mu)), \quad \forall k \in \mathbb{K}. \quad (5)$$

Note that in the sequel we will drop the explicity dependence on the spatial variable $x$ and use the notation $y^k(\mu) = y(x,t^k;\mu)$ unless the $x$-dependence is essential. We shall assume — hence the appellation "truth" — that the discretization is sufficiently rich such that $y^k(\mu)$ and $y^{\rm e}(t^k;\mu)$ and hence $s^k(\mu)$ and $s^{\rm e}(t^k;\mu)$ are indistinguishable. The reduced-basis approximation shall be built upon our reference finite element approximation, and the reduced-basis error will thus be evaluated with respect to $y^k(\mu) \in Y$.

We shall further assume that the bilinear form $a$ depends affinely on the

parameter $\mu$ and can be expressed as

$$a(w, v; \mu) = \sum_{q=1}^{Q_a} \Theta_a^q(\mu)\; a^q(w, v), \quad \forall w, v \in Y,\; \forall \mu \in \mathcal{D}, \tag{6}$$

for some (preferably) small integer $Q_a$. Here, the function $\Theta_a^q(\mu) : \mathcal{D} \to \mathbb{R}$ depends on $\mu$, but the continuous form $a^q$ does *not* depend on $\mu$. We note that the assumption of affine parameter dependence (6) holds for many problems with both property (i.e. physical) and geometry parametric variations (Rozza et al., 2008).

We also briefly recall the algebraic equations induced by (4) and (5). We expand $y^k(\mu) = \sum_{n=1}^{\mathcal{N}} \phi_j(x) y_j^k(\mu)$, then $\underline{y}^k(\mu) = [y_1^k(\mu) \dots y_{\mathcal{N}}^k(\mu)]^T \in \mathbb{R}^{\mathcal{N}}$ satisfies

$$(\underline{M} + \Delta t\, \underline{A}(\mu))\, \underline{y}^k(\mu) + \Delta t\, \underline{G}(\underline{y}^k(\mu); \mu) = \underline{M}\, \underline{y}^{k-1}(\mu) + \Delta t\, \underline{F}\, u(t^k),\; \forall k \in \mathbb{K} \tag{7}$$

with initial condition $\underline{y}^0(\mu) = 0$; we then evaluate the output from

$$s^k(\mu) = \underline{L}^T \underline{y}^k(\mu), \quad \forall k \in \mathbb{K}. \tag{8}$$

The elements of the mass and stiffness matrices $\underline{M} \in \mathbb{R}^{\mathcal{N}\times\mathcal{N}}$ and $\underline{A}(\mu) \in \mathbb{R}^{\mathcal{N}\times\mathcal{N}}$ are given by $\underline{M}_{i,j} = m(\phi_j, \phi_i),\; 1 \le i, j \le \mathcal{N}$ and $\underline{A}_{i,j}(\mu) = a(\phi_j, \phi_i; \mu)$, $1 \le i, j \le \mathcal{N}$, respectively; the elements of the nonlinear term are given by $\underline{G}_i(\underline{y}^k(\mu); \mu) = \int_\Omega g(y^k(\mu); x; \mu)\, \phi_i,\; 1 \le i \le \mathcal{N}$; and the elements of the load vector $\underline{F} \in \mathbb{R}^{\mathcal{N}}$ are given by $\underline{F}_i = f(\phi_i),\; 1 \le i \le \mathcal{N}$.

**Example 1** (*A nonlinear reaction diffusion problem*). We consider a single one-step reaction of a reacting mixture in the region $\Omega = [0, 1]$. The combustion model is given by the PDE (Adjerid and Flaherty, 1986; Kapila, 1983)

$$\frac{\partial T(x,t)}{\partial t} = \alpha \frac{\partial^2 T(x,t)}{\partial x^2} + \mathrm{Da}\,(1 - T(x,t))\, e^{-\gamma/(T(x,t)+1)} \tag{9}$$

with initial condition $T(x, t = 0) = 0$ and boundary conditions $T(x = 0, t) = T(x = 1, t) = 0$. Here, $T(x, t)$ is the temperature at position $x$ and time $t$, $\alpha$ is the thermal diffusivity, Da is the Damköhler number, and $\gamma$ is the Arrhenius number.

The governing equation (9) depends on three parameters; we may thus define the input parameter vector $\mu = [\mu_1, \mu_2, \mu_3] \equiv [\alpha, \mathrm{Da}, \gamma]$. We next derive the weak formulation of (9) and discretize in time using Euler-Backward and in space using finite elements. The equation then assumes the form (4) with $m(w, v) = \int w\, v\, d\Omega$, $a(w, v; \mu) = \alpha \int \frac{\partial w}{\partial x} \frac{\partial v}{\partial x}\, d\Omega$, $f(v) = 0$, and the nonlinearity is given by $g(w; \mu) = \mathrm{Da}\,(1 - w)\, e^{-\gamma/(w+1)}$. We note that $a(w, v; \mu)$ trivially satisfies the affine parameter dependence with $Q_a = 1$: $\Theta_a^1(\mu) = \alpha$ and $a^1(w, v) = \int \frac{\partial w}{\partial x} \frac{\partial v}{\partial x}\, d\Omega$.

### *2.2. Empirical Interpolation Method*

The empirical interpolation method (EIM), introduced in (Barrault et al., 2004), serves to construct affine approximations of parameter dependent non-affine or nonlinear functions. The method is frequently applied in reduced basis approximations of parametrized partial differential equations (Grepl et al., 2007); an affine approximation of the operator allows an "offline-online" computational procedure and is thus crucial for efficiency.

#### *2.2.1. Motivation*

We begin by motivating the need for the EIM. To this end, we suppose that we are given a reduced basis space $W_N^y = \mathrm{span}\{\zeta_n,\ 1 \le n \le N\}$, where the $\zeta_n,\ 1 \le n \le N$, are the basis functions. If we were to follow the classical recipe, the reduced basis approximation would be obtained by a

standard Galerkin projection: given $\mu \in \mathcal{D}$, the reduced basis approximation $y_N^k(\mu) \in W_N^y$ to $y^k(\mu) \in Y$ is the solution of

$$m(y_N^k(\mu), v) + \Delta t \; a(y_N^k(\mu), v; \mu) + \Delta t \int_\Omega g(y_N^k(\mu); x; \mu)\, v \\ = m(y_N^{k-1}(\mu), v) + \Delta t \; f(v) \; u(t^k), \; \forall v \in W_N^y, \; \forall k \in \mathbb{K}, \quad (10)$$

with initial condition $y_N(t^0; \mu) = 0$. We note that, given a new parameter value $\mu$, the terms involving the bilinear and linear forms $m$, $a$, and $f$ can be efficiently evaluated in an offline-online computational procedure (Rozza et al., 2008). However, the nonlinear term $\int_\Omega g(y_N^k(\mu); x; \mu)\, v$ must be evaluated online for every new parameter value; the operation count for the online stage will thus scale as $O(\mathcal{N})$, where $\mathcal{N}$ is the dimension of the underlying finite element truth approximation. Despite the dimension reduction $N \ll \mathcal{N}$, the online cost to evaluate the reduced basis approximation will thus be comparable to the cost to evaluate the truth approximation. This is the reason why most model order reduction techniques for nonlinear problem do not result in computational savings compared to the underlying high-dimensional approximation (Rathinam and Petzold, 2003).

The EIM allows us to completely decouple the evaluation of the reduced basis approximation from the truth approximation. We also note that other approaches to resolve this problem have been proposed previously, see e.g. (Astrid, 2004; Romijn et al., 2008). Recently, the EIM has also been applied in combination with the Proper Orthogonal Decomposition in (Chaturantabut and Sorensen, 2010); also see (Lass and Volkwein, 2011) for a comparison of the two approaches.

*2.2.2. Function Interpolation*

The basic idea of the EIM is to approximate the nonlinear function $g(y^k(\mu); x; \mu),\ \forall k \in \mathbb{K}$, by an affine combination of precomputed basis functions. To this end, we first define the EIM approximation space $W_M^g = \text{span}\{q_j,\ 1 \le j \le M\}$ of dimension $M$, where the $q_j$ are – in essence – precomputed snapshots of the nonlinear parameter dependent function. Given $W_M^g$, we construct an approximation $g_M^{y^k}(x;\mu) \in W_M^g,\ \forall k \in \mathbb{K}$, to the nonlinear function $g(y^k(\mu); x; \mu),\ \forall k \in \mathbb{K}$, as a linear combination of the EIM basis functions, i.e., we have

$$g_M^{y^k}(x;\mu) = \sum_{j=1}^{M} \varphi_{M\,j}^k(\mu)\, q_j(x). \tag{11}$$

The coefficients $\varphi_{M\,j}^k(\mu)$ are determined through the interpolation condition: the interpolant and the nonlinear function have to be identical at the EIM interpolation points $T_M^g = \{x_1^g, x_2^g, \ldots, x_M^g\}$, a set of judiciously selected points in the spatial domain. More specifically, we obtain the coefficients $\varphi_{M\,j}^k(\mu)$ by solving the linear system

$$\sum_{j=1}^{M} \underline{B}_{i\,j}^M \varphi_{M\,j}^k(\mu) = g(y^k(x_i^g;\mu); x_i^g; \mu), \quad 1 \le i \le M,\ \forall k \in \mathbb{K}, \tag{12}$$

where the nodal value matrix is defined as $\underline{B}_{i,j}^M = q_j(x_i^g),\ 1 \le i,j \le M$. Note that the left hand side of (12) is identical to $g_M^{y^k}(x_i^g;\mu)$.

It remains to construct the basis $W_M^g$ and set of interpolation points $T_M^g$. This construction is based on a POD/Greedy selection process which is summarized in Algorithm 1 and explained in detail below. We present the procedure described in (Grepl, 2012); see (Maday et al., 2009) for the linear nonaffine case.

Before explaining the steps in Algorithm 1, we need to introduce a finite train sample $\Xi_{\text{train}} \subset \mathcal{D}$ of size $|\Xi_{\text{train}}|$ which shall serve as our computational surrogate for $\mathcal{D}$. We also require the function $\text{POD}_{L^2(\Omega)}(\{w^k(\mu), 1 \leq k \leq K\})$, which returns the largest POD mode, $\chi_1$, with respect to the $(\cdot,\cdot)_{L^2(\Omega)}$ inner product. Here, $L^2(\Omega)$ is the space of square integrable functions over $\Omega$. We use the method of snapshots to obtain $\chi_1$ (Sirovich, 1987): to this end, we solve the eigenvalue problem $C\psi^i = \lambda^i \psi^i$ for $(\psi^1 \in \mathbb{R}^K, \lambda^1 \in \mathbb{R})$ associated with the largest eigenvalue of $C$, where $C_{ij} = (w^i(\mu), w^j(\mu))_{L^2(\Omega)},\ 1 \leq i, j \leq K$; we then obtain the first POD mode from $\chi_1 = \sum_{k=1}^K \psi_k^1 \, w^k(\mu)$.

The POD/Greedy-EIM procedure in Algorithm 1 proceeds by induction: we first choose randomly an initial parameter value $\mu_1 \in \mathcal{D}$ and calculate the first POD mode, $\xi_1(x)$, of the time-history of the nonlinear function evaluated at $y^k(\mu_1)$ in step 2. In step 3 and 4 we choose the first interpolation point, $x_1^g$, to be the spatial point where $\xi_1(x)$ is maximal, the first basis function, $q_1(x)$, to be the normalized POD mode $\xi_1(x)/\xi_1(x_1^g)$, and the nodal value matrix, $\underline{B}^1$, is simply $q_1(x)$ evaluated at $x_1^g$. We thus obtain a one-dimensional EIM approximation to the nonlinear function.

Given the current EIM approximation, we perform a greedy search over $\Xi_{\text{train}}$ in step 6 to find the parameter value where the $L^\infty(\Omega)$ norm of the interpolation error over time is maximal, i.e., where the approximation is worst. We then calculate the largest POD mode, $\xi_{M+1}(x)$, of the time-history of the interpolation error at this parameter value in step 7 and 8. Note that we perform a POD on the interpolation error instead of the nonlinear function itself in order to consistently "add" new information at each step of the POD/Greedy procedure. Given $\xi_{M+1}(x)$, we evaluate the next interpolation

point and basis function: in steps 9 and 10 we calculate the residual vector $r_{M+1}(x)$, in step 11 we set the next interpolation point, $x^g_{M+1}$, to be the spatial point where the residual is maximal, and in step 12 we set the next basis function, $q_{M+1}(x)$, to be the normalized residual. We then expand the EIM space in step 13 and update the nodal value matrix in step 14. Finally, we increment $M$ and go back to step 6 if $M \leq M_{\max} - 1$. In general, we may also specify a desired error tolerance, $\epsilon_{\text{tol,min}}$, and stop the procedure as soon as $\max_{\mu \in \Xi_{\text{train}}} \sum_{k=1}^{K} \|g(y^k(x;\mu);x;\mu) - g_M^{y^k}(x;\mu)\|_{L^\infty(\Omega)} \leq \epsilon_{\text{tol,min}}$ is satisfied; $M_{\max}$ is then indirectly determined through the stopping criterion.

Note that by construction, the EIM space satisfies $W_M^g = \text{span}\{q_m(x),\ 1 \leq m \leq M\} = \text{span}\{\xi_m(x),\ 1 \leq m \leq M\}$. Furthermore, the nodal value matrix $\underline{B}^M$, $1 \leq M \leq M_{\max}$, is lower triangular and hence computation of the EIM coefficients $\varphi^k_{M\,j}$ in (12) is an $\mathcal{O}(M^2)$ operation per timestep. It can be shown that the interpolation process is well-defined. For more details on the EIM including an a priori and a posteriori error analysis for the linear nonaffine case we refer the interested reader to (Barrault et al., 2004; Grepl et al., 2007; Maday et al., 2009; Eftang et al., 2010).

We note that we do require the truth solution for all $\mu$ in $\Xi_{\text{train}}$ in Algorithm 1 to generate the EIM interpolation points and space. The overall computational cost is thus very high and the procedure only viable if there is a clear demand for real-time response or a many query context.

### *2.3. Reduced Basis Method*

In Section 2.2.1 we briefly introduced a straightforward reduced basis approximation to the nonlinear problem (4). We now return to this discussion and show that we can devise a very efficient offline-online computational

**Algorithm 1:** POD/Greedy-EIM Algorithm

1. specify $\Xi_{\text{train}} \subset \mathcal{D}$ , $M_{\max}$, $\mu_1 \in \mathcal{D}$ (arbitrary).
2. $\xi_1(x) = \text{POD}_{L^2(\Omega)}(\{g(y^k(x;\mu_1);x;\mu_1), 1 \le k \le K\})$.
3. set $M = 1$, $x_1^g = \arg\sup_{x\in\Omega} |\xi_1(x)|$ and $q_1(x) = \xi_1(x)/\xi_1(x_1^g)$
4. set $W_1^g \equiv \text{span}\{q_1\}$ and $\underline{B}_{1,1}^1 = q_1(x_1^g) = 1$.
5. **while** $M \le M_{\max} - 1$ **do**
6. $\mu_{M+1} = \arg\max_{\mu\in\Xi_{\text{train}}} \sum_{k=1}^K \|g(y^k(x;\mu);x;\mu) - g_M^{y^k}(x;\mu)\|_{L^\infty(\Omega)}$,
   where $g_M^{y^k}$ is calculated from (11) and (12);
7. $e_{M,\text{EIM}}^k(\mu) = g(y^k(\mu_{M+1});x;\mu_{M+1}) - g_M^{y^k}(x;\mu_{M+1})$, $\forall k \in \mathbb{K}$;
8. $\xi_{M+1}(x) = \text{POD}_{L^2(\Omega)}(\{e_{M,\text{EIM}}^k(\mu_{M+1}), 1 \le k \le K\})$;
9. solve for $\sigma_j^M$ from $\sum_{j=1}^M \sigma_j^M\, q_j(x_i^g) = \xi_{M+1}(x_i^g),\ 1 \le i \le M$;
10. set $r_{M+1}(x) \equiv \xi_M(x) - \sum_{j=1}^M \sigma_j\, q_j(x)$;
11. set $x_{M+1}^g \equiv \arg\sup_{x\in\Omega} |r_{M+1}(x)|$;
12. set $q_{M+1}(x) \equiv r_{M+1}(x)/r_{M+1}(x_{M+1}^g)$;
13. $W_{M+1}^g \leftarrow W_M^g \cup \text{span}\{q_{M+1}(x)\}$;
14. $\underline{B}_{i,j}^{M+1} = q_j(x_i^g), \quad 1 \le i,j \le M+1$;
15. $M \leftarrow M + 1$;
16. **end**

strategy by combining the EIM with the reduced basis approximation.

*2.3.1. Approximation*

We suppose that we are given the nested reduced basis spaces

$$W_N^y = \text{span}\{\zeta_n,\ 1 \le n \le N\}, \quad 1 \le N \le N_{\max}, \tag{13}$$

where the $\zeta_n,\ 1 \le n \le N$, are mutually orthogonal basis functions. We comment on the adaptive procedure for constructing the basis functions in Section 2.3.3.

Given the nested EIM space $W_M^g = \text{span}\{q_1, \ldots, q_M\},\ 1 \le M \le M_{\max}$, and nested set of interpolation points $T_M^g = \{x_1^g, \ldots, x_M^g\},\ 1 \le M \le M_{\max}$, our reduced basis approximation $y_{N,M}^k(\mu)$ to $y^k(\mu)$ is obtained by a standard Galerkin projection: given $\mu \in \mathcal{D}$, $y_{N,M}^k(\mu) \in W_N^y$ satisfies

$$\begin{aligned} m(y_{N,M}^k(\mu), v) + \Delta t\ a(y_{N,M}^k(\mu), v; \mu) + \Delta t \int_\Omega g_M^{y_{N,M}^k}(x;\mu)\ v \\ = m(y_{N,M}^{k-1}(\mu), v) + \Delta t\, f(v)\, u(t^k), \quad \forall v \in W_N^y,\ \forall k \in \mathbb{K}, \end{aligned} \tag{14}$$

with initial condition $y_{N,M}^0(\mu) = 0$. We then evaluate the output approximation, $s_{N,M}^k(\mu) \in \mathbb{R}$, from

$$s_{N,M}^k(\mu) = \ell(y_{N,M}^k(\mu)), \quad \forall k \in \mathbb{K}. \tag{15}$$

Comparing (14) and (10) we observe that the nonlinearity $g(y_N^k(\mu); x; \mu)$ is now replaced by its EIM approximation $g_M^{y_{N,M}^k}(x;\mu)$. Here, $g_M^{y_{N,M}^k}(x;\mu) \in W_M^g$ is given by

$$g_M^{y_{N,M}^k}(x;\mu) = \sum_{i=1}^M \tilde{\varphi}_{M\,i}^k(\mu)\, q_i(x). \tag{16}$$

where the coefficients $\tilde{\varphi}^k_{M\,i}(\mu),\ 1 \le i \le M$, are obtained through the interpolation condition, i.e., the solution of the linear system

$$\sum_{j=1}^{M} \underline{B}^M_{i\,j} \tilde{\varphi}^k_{M\,j}(\mu) = g(y^k_{N,M}(x^g_i;\mu);x^g_i;\mu), \quad 1 \le i \le M,\ \forall k \in \mathbb{K}. \tag{17}$$

Note that the space $W^g_M$ is constructed based on $g(y^k(\mu);x;\mu)$ and not $g(y^k_{N,M}(\mu);x;\mu)$. However, as $N$ and $M$ increase the reduced basis solution $y^k_{N,M}(\mu)$ converges to the truth solution $y^k(\mu)$ very rapidly. We thus expect $g(y^k_{N,M}(\mu);x;\mu)$ to be well approximated in $W^g_M$. We shall observe the (in fact, exponential) convergence when we discuss numerical results in Section 4.

We note that the need to incorporate the empirical interpolation method into the reduced basis approximation only exists for high-order polynomial or non-polynomial nonlinearities (Grepl et al., 2007). If $g$ is a low-order (or at most quadratically) polynomial nonlinearity in $y^k(\mu)$, we can expand the nonlinear terms into their power series and develop an efficient, i.e., online $\mathcal{N}$-independent, offline-online computational decomposition using the standard Galerkin procedure (Veroy and Patera, 2005; Veroy et al., 2003). We also note that for linear or nonlinear problems with a non-affine parameter dependence the EIM is always required to develop an efficient offline-online computational procedure for the nonaffine terms.

*2.3.2. Computational Procedure*

The EIM allows us to develop an efficient offline-online computational procedure to solve (14). We omit the details here and refer the interested reader to (Grepl et al., 2007; Grepl, 2012). The main idea is to first express

$y^k_{N,M}(\mu)$ as

$$y^k_{N,M}(\mu) = \sum_{n=1}^{N} y^k_{N,Mn}(\mu)\ \zeta_n \tag{18}$$

and choose as test functions $v = \zeta_j,\ 1 \le j \le N$, in (14). We then invoke the affine representation (16) of $g_M^{y^k_{N,M}}$ and (17) to obtain a nonlinear algebraic system of dimension $N$ which we solve at each timestep using a Newton iterative scheme.

During the offline stage we generate the reduced basis space and evaluate several parameter independent quantities — the offline operation count thus depends on $\mathcal{N}$, the dimension of the underlying "truth" finite element approximation space. The operation count in the online stage, however, is (to leading order) $O(MN^2 + N^3)$ per Newton iteration per timestep and thus *independent* of $\mathcal{N}$. Since $N \ll \mathcal{N}$ we expect significant computational savings in the online stage relative to classical discretization and solution approaches. We will confirm these savings in Section 4.

*2.3.3. Adaptive Sampling Procedure*

Given $W_M^g$, $T_M^g$, and $\underline{B}^M$, we invoke a POD/Greedy sampling procedure — a combination of the Proper Orthogonal Decomposition (POD) in time with a Greedy selection procedure in parameter space — to generate $W_N^y$ (Haasdonk and Ohlberger, 2008; Grepl, 2012). We shall use the "best" possible approximation $g_M^{y^k_{N,M}}(x;\mu)$ of $g(y^k_{N,M};x;\mu)$ during the sampling process so as to minimize the error induced by the empirical interpolation procedure, i.e., we set $M = M_{\max}$. The POD/Greedy Algorithm is summarized in Algorithm 2. Here, $\mathrm{POD}_X(\{w^k(\mu), 1 \le k \le K\})$ returns the largest POD mode with respect to the $(\cdot,\cdot)_X = a(\cdot,\cdot;\mu_{\mathrm{ref}})$ inner product,

**Algorithm 2:** POD/Greedy Algorithm

1. Specify $\Xi_{\text{train}} \subset \mathcal{D}$, $N_{\max}$, $\mu_1 \in \mathcal{D}$ (arbitrary).
2. Set $W_0^y = \{0\}$ and $N = 1$.
3. **while** $N \leq N_{\max} - 1$ **do**
4. $\quad e^k_{N,\text{proj}}(\mu_N) = y^k(\mu_N) - \text{proj}_{X,W^y_{N-1}}(y^k(\mu_N))$, $\forall k \in \mathbb{K}$;
5. $\quad W^y_N \leftarrow W^y_{N-1} \cup \text{POD}_X(\{e^k_{N,\text{proj}}(\mu_N),\ 1 \leq k \leq K\})$;
6. $\quad \mu_{N+1} = \arg\max_{\mu \in \Xi_{\text{train}}} |||y^K(\mu) - y^K_{N,M}(\mu)|||/|||y^K(\mu)|||$;
7. $\quad N \leftarrow N + 1$;
8. **end**

where $\mu_{\text{ref}} \in \mathcal{D}$ is a reference parameter value; $\text{proj}_{X,W_N}(w)$ denotes the $X$-orthogonal projection of $w \in X$ onto $W^y_N$; and the energy norm is defined as $|||w^k|||^2 = m(w^k, w^k) + \Delta t \sum_{k'=1}^k a(w^{k'}, w^{k'}; \mu)$.

In general, we may also specify a desired error tolerance, $\epsilon_{\text{tol,min}}$, and stop the procedure as soon as $\max_{\mu \in \Xi_{\text{train}}} |||y^K(\mu) - y^K_{N,M}(\mu)|||/|||y^K(\mu)||| \leq \epsilon_{\text{tol,min}}$ is satisfied; $N_{\max}$ is then indirectly determined through the stopping criterion.

## 3. Nonlinear Reaction-Diffusion Systems

In this section we consider a specific problem belonging to the class of nonlinear reaction-diffusion systems (Smoller, 1994). Reaction-diffusion systems appear in a large number of real-world applications: ranging from Biology, where reaction-diffusion equations characterize the pattern formation

in morphogenesis and mutations in genetics; to Ecology, where they govern predator-prey relation and the spreading of epidemics; to Physiology, where the conduction in nerves and carbon monoxide poisoning is described by reaction-diffusion equations; to Chemistry, probably the most notable application area of reaction-diffusion equations. Furthermore, inherent to these equations and the specific application area are a large number of parameters, which, in general, have a very strong influence on the dynamic behavior of the system, e.g., such as reaction rates in chemistry. The reduced basis method is thus ideally suited for the treatment of parametrized nonlinear reaction-diffusion systems.

We now extend the methodology introduced in the last section to coupled systems of nonlinear equations. We introduced separate reduced basis spaces for each field variable. Furthermore, we employ the EIM to generate an affine approximation of the nonlinear coupling term, thus allowing an efficient offline-online procedure even for the coupled system of nonlinear equations.

### *3.1. Model Problem*

As a specific example, we consider a one-dimensional non-isothermal reaction-diffusion model for the self-ignition of a coal stockpile with Arrhenius type nonlinearity (Schmal et al., 1985; Brooks et al., 1988; Brooks and Glasser, 1986; Brooks et al., 1988; Salinger et al., 1994). In practice this problem arises if large piles of coal are stored, e.g., in harbors, over extended periods of time. As the oxygen in the air reacts with the coal, the pile starts to heat up and can eventually self-ignite if certain conditions — on porosity, oxygen concentration, and coal size — are met. We also note that similar models are used in combustion theory (see Example 1), biology, and in the

description of porous catalysts.

The field variables are the temperature of the reactive medium (here, the coal) normalized by the ambient temperature, $T(x,t) = (\overline{T}(x,t) - \overline{T}_\infty)/\overline{T}_\infty$, and the concentration of the reactantd (here, the oxygen in the air) normalized by the concentration of oxygen in the ambient air, $c(x,t) = (\overline{c}(x,t) - \overline{c}_\infty)/\overline{c}_\infty$. The coupled set of governing equations are given by (Brooks et al., 1988)

$$\frac{\partial T(x,t)}{\partial t} = \nabla^2 T(x,t) + 4.287 \cdot 70000\,(c(x,t)+1)\,e^{-\gamma/(T(x,t)+1)}, \quad (19)$$

$$\frac{\partial c(x,t)}{\partial t} = 0.233\,\nabla^2 c(x,t) - 70000\,(c(x,t)+1)\,e^{-\gamma/(T(x,t)+1)}, \quad (20)$$

with initial conditions

$$T(x,t=0) = T_0 = 0, \quad (21)$$

$$c(x,t=0) = c_0 = \frac{1}{(3x+1)^2} - 1. \quad (22)$$

The boundary conditions are

$$\begin{aligned} T(x,t)|_{x=0} &= 0, & T(x,t)|_{x=1} &= 0, \\ c(x,t)|_{x=0} &= 0, & \left.\frac{\partial c(x,t)}{\partial x}\right|_{x=1} &= 0. \end{aligned} \quad (23)$$

A sketch of the distribution of temperature and concentration for $t > 0$ is shown in Figure 1. Here, $x \in \Omega \subset \mathbb{R}^1$ is the spatial coordinate and $\Omega \equiv [0,1]$ is the spatial domain. Note that $x = 0$ corresponds to the top of the pile at which $T(x,t)$ and $c(x,t)$ are equal to the the ambient temperature and concentration, respectively; and $x = 1$ corresponds to the bottom of the pile at which $T(x,t)$ is equal to the ground (ambient) temperature, and the concentration gradient is zero. The one-dimensional model accounts only for the vertical variation in the state variable; the length and width of the coal

pile are assumed to be much larger than its height. The outputs of interest, $s_1$ and $s_2$, are the temperature and concentration at $x = 0.2$ both shifted by one, respectively.

We only consider one parameter, the Arrhenius number $\gamma$, in this model problem. We assume that $\gamma$ varies in the range $12 \leq \gamma \leq 12.6$ (Brooks et al., 1988); we thus have $\mu \equiv \gamma \in \mathcal{D} \equiv [12, 12.6] \subset \mathbb{R}^{P=1}$. Although the parametric variation is quite small, we will see that the system exhibits a very interesting dynamical behavior in terms of complex oscillatory patterns for this parameter range.

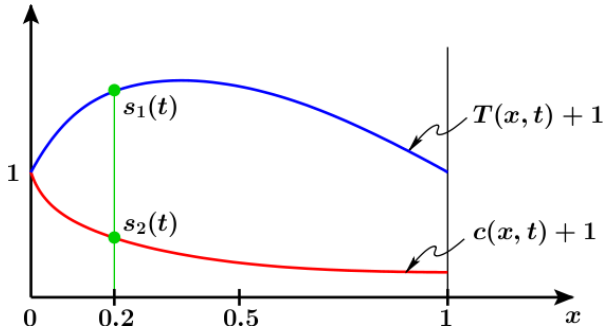


Figure 1: Sketch of temperature distribution and concentration for the model problem for $t > 0$ (Note that both quantities are shifted by 1).

### *3.2. Truth Approximation*

We next derive the weak form of the governing equations (19) and (20) and discretize in time using Euler-Backward. We also introduce the linear finite element truth approximation subspaces $Y_T \equiv \{v | v \in H^1(\Omega), v = 0|_{x=0,1}\}$ and $Y_c \equiv \{v | v \in H^1(\Omega), v = 0|_{x=0}\}$ both of dimension $\mathcal{N} = 501$, where $H^1(\Omega)$ is a suitable Hilbert space and $\Omega \equiv [0, 1]$ is the spatial domain. We associated to $Y_T$ and $Y_c$ a set of piecewise linear (over each element) basis functions

$\phi_i(x),\ 1 \le i \le \mathcal{N}$ (note that we use the same spatial discretization for $Y_T$ and $Y_c$ and they thus share the same basis). We shall consider the time interval $\bar{I} = [0, 6]$ and a timestep $\Delta t = 1\,\mathrm{E}{-3}$; we thus have $K = 6000$. Our truth approximation is thus: Given $\mu \in \mathcal{D}$, find $T^k(\mu) \in Y_T$ and $c^k(\mu) \in Y_c$ such that[2]

$$\begin{aligned} &m(T^k(\mu), v_T) + \Delta t\, a(T^k(\mu), v_T) \\ &\qquad - \Delta t \cdot 4.287 \cdot 70000 \int_\Omega (c^k(\mu) + 1)\, e^{-\mu/(T^k(\mu)+1)}\, v_T \\ &\qquad\qquad = m(T^{k-1}(\mu), v_T), \quad \forall v_T \in Y_T,\ \forall k \in \mathbb{K} \end{aligned} \tag{24}$$

$$\begin{aligned} &m(c^k(\mu), v_c) + \Delta t \cdot 0.233\, a(c^k(\mu), v_c) \\ &\qquad + \Delta t \cdot 70000 \int_\Omega (c^k(\mu) + 1)\, e^{-\mu/(T^k(\mu)+1)}\, v_c \\ &\qquad\qquad = m(c^{k-1}(\mu), v_c), \quad \forall v_c \in Y_c,\ \forall k \in \mathbb{K} \end{aligned} \tag{25}$$

with inital conditions $m(T^0(\mu), v_T) = m(T_0, v_T),\ \forall v_T \in Y_T,\ m(c^0(\mu), v_c) = m(c_0, v_c),\ \forall v_c \in Y_c$. We then evaluate the outputs from

$$s_1^k(\mu) = \ell(T^k(\mu)) + 1, \qquad \forall k \in \mathbb{K}, \tag{26}$$

and

$$s_2^k(\mu) = \ell(c^k(\mu)) + 1, \quad \forall k \in \mathbb{K}. \tag{27}$$

Here, $\ell(v) = \int_\Omega \delta(x - 0.2)\, v$, where $\delta(x)$ is the Dirac delta function, and the bilinear forms are given by

$$m(w, v) = \int_\Omega w\, v, \quad a(w, v) = \int_\Omega \frac{\partial w}{\partial x}\, \frac{\partial v}{\partial x}. \tag{28}$$

[2]Note that we use our usual notation here: $T^k(\mu) = T(x, t^k; \mu)$ and $c^k(\mu) = c(x, t^k; \mu)$.

We also define the nonlinearity $g$ as

$$g(c^k(\mu), T^k(\mu); \mu) = (c^k(\mu) + 1)\, e^{-\mu/(T^k(\mu)+1)}. \tag{29}$$

The algebraic equations induced by (24) and (25) directly follow from the discussion in Section 2.1 and are therfore omitted. Note, however, that we now obtain a coupled system of nonlinear equations which have to be solved at each timestep using a Newton iterative scheme.

*3.2.1. Numerical Results*

We present results for the truth approximation. In Figure 2, we plot the outputs $s_1$ and $s_2$ for $\mu = 12.0$ over (discrete) time. The sharp peak in the temperature output $s_1$ and corresponding drop in the concentration output $s_2$ indicates the ignition of the system. After the ignition, the system goes into a stable steady-state solution. In Figure 3 we show the corresponding output plots for $\mu = 12.5$; we first note that the ignition occurs at a later point in time and that the maximum temperature reached is higher. For this parameter value the system does not return to a steady-state solution, but converges to a period 1 limit cycle. Finally, we present in Figure 4 the output plots for $\mu = 12.58$. Again, the time of ignition occurs later and the maximum temperature is higher than before. Furthermore, the system converges to a limit cycle with mixed mode oscillations. To clearly visualize the limit cycles, we show in Figures 5 and 6 the phase plots for the solutions corresponding to the two parameter values $\mu = 12.5$ and $\mu = 12.58$ without the transient behavior, respectively. We can clearly see the period 1 limit cycle for $\mu = 12.5$; as $\mu$ is increased, a period doubling cascade occurs leading to the mixed mode oscillations for $\mu = 12.58$.

We note that there is a certain critical parameter value $\mu_{\text{crit}}$: if $\mu < \mu_{\text{crit}}$ the system goes into a stable steady-state solution after the first ignition, whereas if $\mu \geq \mu_{\text{crit}}$ the system converges to a limit cycle after the first ignition. We numerically identified this critical value to be approximately $\mu_{\text{crit}} \approx 12.24$.

The systems clearly exhibits a very complex dynamic behaviour with a strong dependence on the parameter $\mu$. Approximating such a systems with a reduced order model over parameter and time is certainly a very challenging task.

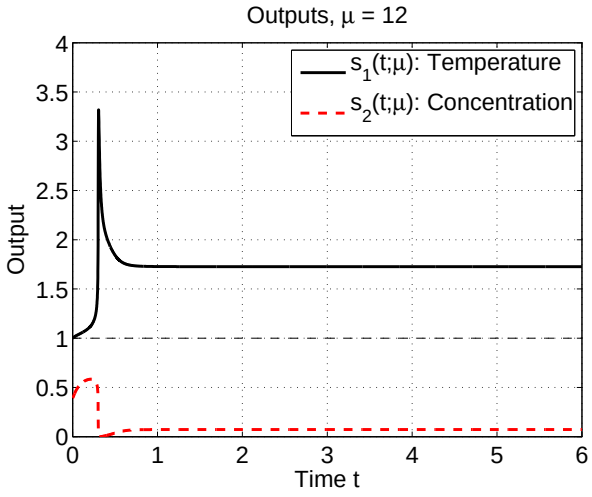


Figure 2: Outputs $s_1(t;\mu)$ and $s_2(t;\mu)$ for $\mu = 12.0$ as a function of time.

### *3.3. Reduced Basis Approximation*

We develop the reduced basis approximation for the coupled system of nonlinear equations (24) and (25) by generalizing the approach described in Section 2.3.1. We first introduce a finite train sample $\Xi_{\text{train}} \subset \mathcal{D}$ and solve and store the solutions $T^k(\mu)$ and $c^k(\mu)$ to (24) and (25) for all $\mu \in \Xi_{\text{train}}$

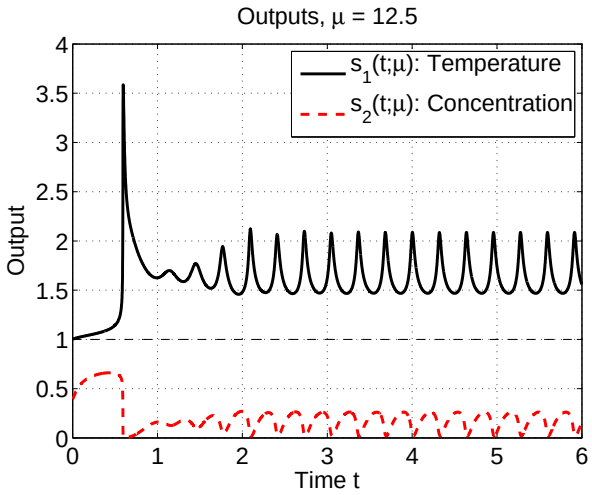


Figure 3: Outputs $s_1(t;\mu)$ and $s_2(t;\mu)$ for $\mu = 12.5$ as a function of time.

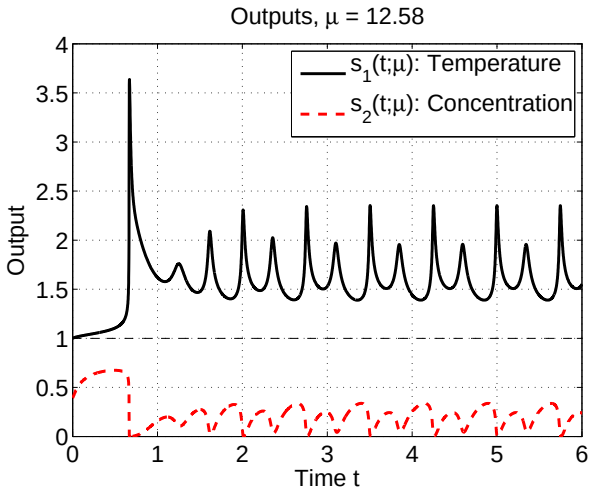


Figure 4: Outputs $s_1(t;\mu)$ and $s_2(t;\mu)$ for $\mu = 12.58$ as a function of time.

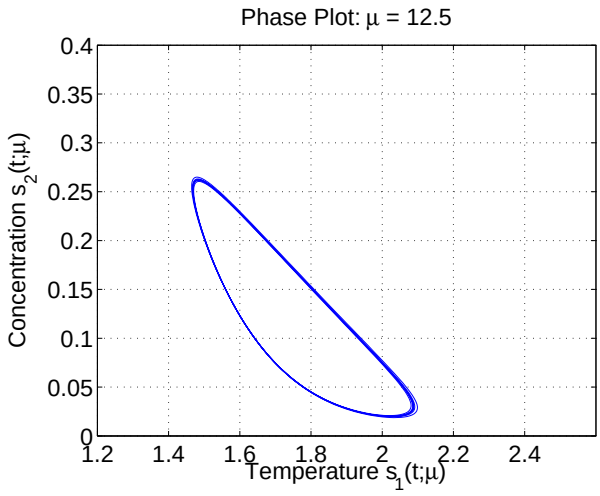


Figure 5: Limit Cycls in phase plane ($s_1(t;\mu)$ vs. $s_2(t;\mu)$) for $\mu = 12.5$ without transition from initial condition.

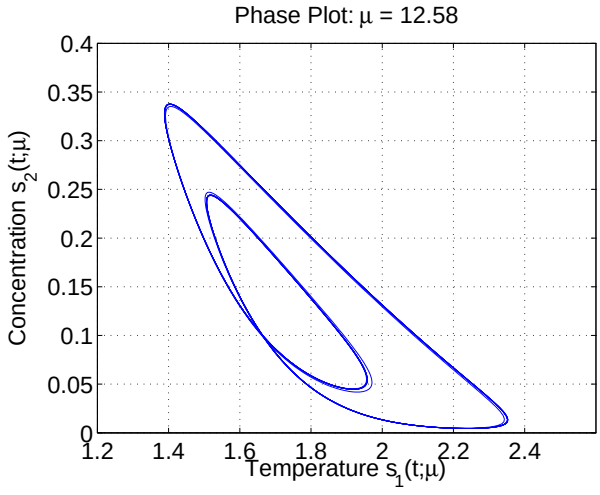


Figure 6: Limit Cycles in phase plane ($s_1(t;\mu)$ vs. $s_2(t;\mu)$) for $\mu = 12.58$ without transition from initial condition.

and for all $k \in \mathbb{K}$, respectively. Given $g(c^k(\mu), T^k(\mu); \mu)$ in (29), we generate the nested EIM spaces $W_M^g = \text{span}\{q_1, \ldots, q_M\},\ 1 \le M \le M_{\max}$, and nested set of interpolation points $T_M^g = \{x_1^g, \ldots, x_M^g\},\ 1 \le M \le M_{\max}$, according to the procedure described in Section 2.2.2. Note that the nonlinearity depends on both field variables and we thus have to generalize the definition of the interpolant (8) and of the EIM coefficients (7): the approximation $g_M^{c^k,T^k}(x;\mu)$ to $g(c^k(\mu), T^k(\mu); \mu)$ is given by

$$g_M^{c^k,T^k}(x;\mu) = \sum_{m=1}^{M} \varphi_{Mm}^k(\mu) q_m(x) \tag{30}$$

where the coefficients $\varphi_{Mm}^k(\mu)$ are determined from

$$\sum_{j=1}^{M} \underline{B}_{ij}^M \varphi_{Mj}^k(\mu) = g(c^k(x_i^g;\mu), T^k(x_i^g;\mu);\mu), \quad 1 \le i \le M \tag{31}$$

and $\underline{B}_{ij}^M = q_j(x_i^g),\ 1 \le i, j \le M,\ 1 \le M \le M_{\max}$. Given $W_M^g$ and $T_M^g$, we next define the associated nested reduced-basis spaces for the temperature

$$W_{N_T}^T = \text{span}\{\zeta_{T,m},\ 1 \le n \le N_T\}, \quad 1 \le N_T \le N_{T,\max}, \tag{32}$$

and the concentration

$$W_{N_c}^c = \text{span}\{\zeta_{c,m},\ 1 \le n \le N_c\}, \quad 1 \le N_c \le N_{c,\max}, \tag{33}$$

according to the adaptive procedure described in Section 2.3.3. We introduce separate spaces for temperature and concentration with possibly different dimensions $N_T$ and $N_c$, respectively.

Our reduced-basis approximation is then: given $\mu \in \mathcal{D}$, $T_{N,M}^k(\mu) \in W_{N_T}^T$

and $c^k_{N,M}(\mu) \in W^c_{N_c}$ satisfy

$$m(T^k_{N,M}(\mu), v_T) + \Delta t\, a(T^k_{N,M}(\mu), v_T) \\ - \Delta t \cdot 4.287 \cdot 70000 \int_\Omega g_M^{c^k_{N,M}, T^k_{N,M}}(x;\mu)\, v_T \\ = m(T^{k-1}_{N,M}(\mu), v_T), \quad \forall v_T \in W^T_{N_T},\ \forall k \in \mathbb{K} \quad (34)$$

$$m(c^k_{N,M}(\mu), v_c) + \Delta t \cdot 0.233\, a(c^k_{N,M}(\mu), v_c) \\ + \Delta t \cdot 70000 \int_\Omega g_M^{c^k_{N,M}, T^k_{N,M}}(x;\mu)\, v_c \\ = m(c^{k-1}_{N,M}(\mu), v_c), \quad \forall v_c \in W^c_{N_c},\ \forall k \in \mathbb{K} \quad (35)$$

with inital conditions determined from $m(T^0_{N,M}(\mu), v_T) = m(T_0, v_T),\ \forall\, v_T \in W^T_{N_T}$, and $m(c^0_{N,M}(\mu), v_c) = m(c_0, v_c),\ \forall\, v_c \in W^c_{N_c}$; here, $g_M^{c^k_{N,M}, T^k_{N,M}}(x;\mu)$ is given by

$$g_M^{c^k_{N,M}, T^k_{N,M}}(x;\mu) = \sum_{m=1}^{M} \tilde{\varphi}^k_{Mm}(\mu) q_m(x) \quad (36)$$

where the coefficients $\tilde{\varphi}^k_{Mm}(\mu)$ are determined from

$$\sum_{j=1}^{M} \underline{B}^M_{ij} \tilde{\varphi}^k_{Mj}(\mu) = g(c^k_{N,M}(x^g_i;\mu), T^k_{N,M}(x^g_i;\mu);\mu), \quad 1 \le i \le M, \quad (37)$$

and $\underline{B}^M_{ij} = q_j(x^g_i),\ 1 \le i, j \le M,\ 1 \le M \le M_{\max}$. Finally, we evaluate the outputs from

$$s^k_{1,N,M}(\mu) = \ell(T^k_{N,M}(\mu)) + 1, \quad \forall k \in \mathbb{K}, \quad (38)$$

and

$$s^k_{2,N,M}(\mu) = \ell(c^k_{N,M}(\mu)) + 1, \quad \forall k \in \mathbb{K}. \quad (39)$$

The offline-online computational procedure directly follows from the scalar case briefly discussed in Section 2.3.2. We thus omit the details and only

summarize the computational cost: the operation count in the online stage is $O(MN^2 + N^3)$ per Newton step per timestep, where $N = N_T + N_c$. Again, the operation count in the online stage is thus *independent* of $\mathcal{N}$.

## 4. Numerical Results

We now present numerical results for the model problem introduced in Section 3.1. We choose for $\Xi_{\text{train}} \subset \mathcal{D}$ a regular grid of 15 parameter points over $\mathcal{D}$ and we take $\mu_1^g = 12$. Next, we pursue the POD/Greedy-EIM procedure in Algorithm 1 to construct $W_M^g$, $T_M^g$, and $\underline{B}^M$, $1 \leq M \leq M_{\max}$, with $M_{\max} = 36$. We plot the convergence of the error $\varepsilon_{M,\max}^g = \max_{\mu \in \Xi_{\text{train}}} \sum_{k=1}^K \|g(c^k(\mu), T^k(\mu); \mu) - g_M^{c^k, T^k}(x; \mu)\|_{L^\infty(\Omega)}$ in Figure 7.

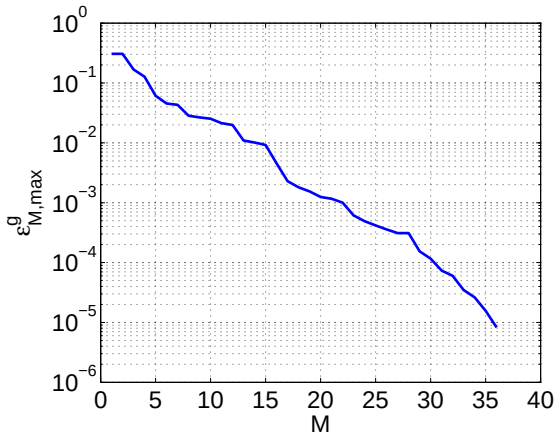


Figure 7: Convergence results for EIM interpolation error.

We next consider to the reduced basis approximation and construct the reduced basis spaces $W_{N_T}^T$ and $W_{N_c}^c$ according to the POD/Greedy procedure in Algorithm 2 using the train sample $\Xi_{\text{train}}$. In Figure 8(a) and (b) we plot, as a function of $N_T$, $N_c$, and $M$, the maximum relative errors

$\epsilon^T_{N,M,\max,\mathrm{rel}}$ in the temperature and $\epsilon^c_{N,M,\max,\mathrm{rel}}$ in the concentration, respectively; here $\epsilon^T_{N,M,\max,\mathrm{rel}} = \max_{\mu\in\Xi_{\mathrm{Test}}} |||T^K(\mu) - T^K_{N,M}(\mu)|||/|||T^K(\mu_T)|||$, where $\mu_T \equiv \arg\max_{\mu\in\Xi_{\mathrm{Test}}} |||T^K(\mu)|||$ (similarly for $\epsilon^c_{N,M,\max,\mathrm{rel}}$) and $\Xi_{\mathrm{Test}}$ is a test sample of size 25 (a regular grid in $\mathcal{D}$; note that the test and train samples are, of course, different). We observe that the reduced basis approximation converges very rapidly. We also note the "plateau" in the curves for $M$ fixed and the "drops" in the $N_T, N_c \to \infty$ asymptotes as $M$ increases: for fixed $M$ the error due to the coefficient function approximation will ultimately dominate for large $N_T$ and $N_c$; increasing $M$ renders the coefficient function approximation more accurate, which in turn leads to a drop in the error. We further note that the separation points, or "knees," of the $N_T$-$M$-convergence curves (resp. $N_c$-$M$-convergence curves) reflect a balanced contribution of both error terms; neither $N_T$ (resp. $N_c$) nor $M$ limit the convergence of the reduced basis approximation.

We turn to the output estimate and present, in Figure 9(a) and (b), as a function of $N_T$, $N_c$, the maximum relative output errors $\epsilon^{s_1}_{N,M,\max,\mathrm{rel}}$ and $\epsilon^{s_2}_{N,M,\max,\mathrm{rel}}$, respectively; here, $\epsilon^s_{N,M,\max,\mathrm{rel}}$ is the maximum over $\Xi_{\mathrm{Test}}$ of $\max_{k\in\mathbb{K}} |s^k(\mu) - s^k_{N,M}(\mu)|/s_{\max}(\mu)$, where $s_{\max}(\mu) \equiv \max_{k\in\mathbb{K}} |s^k(\mu)|$. We observe also very rapid convergence of the reduced basis output approximation. The output error shows the same behavior as the error in the energy norm: the $M$-asymptotes level off at a lower and lower error as $M$ increases. To obtain a maximum relative error in both outputs of less than 1%, we require approximately $M = 30$, $N_T = 13$, and $N_c = 13$.

In Table 1 we present, as a function of $N = N_T = N_c$ and $M$, the average online computational times to calculate $s^k_{1,N,M}(\mu)$ and $s^k_{2,N,M}(\mu)$ for

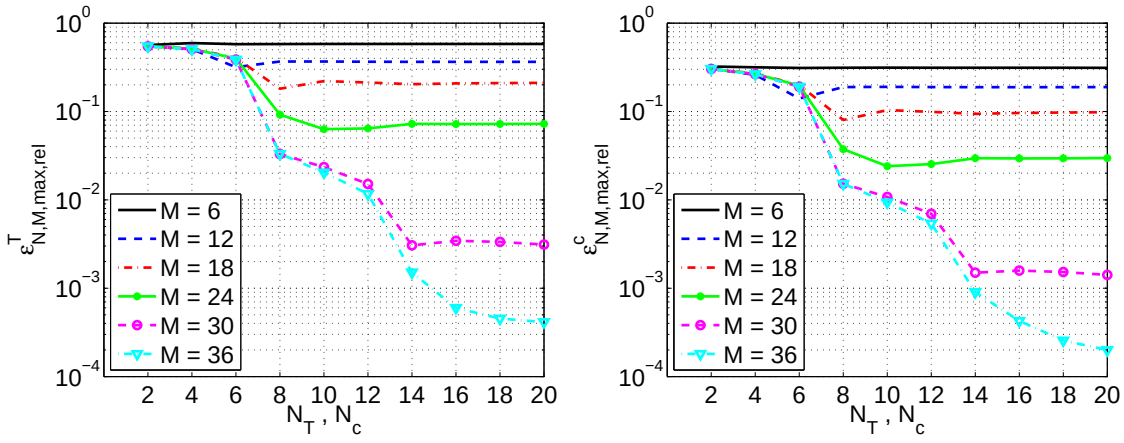


(a) (b)

Figure 8: Convergence of the reduced basis approximation: maximum relative error in the energy norm.

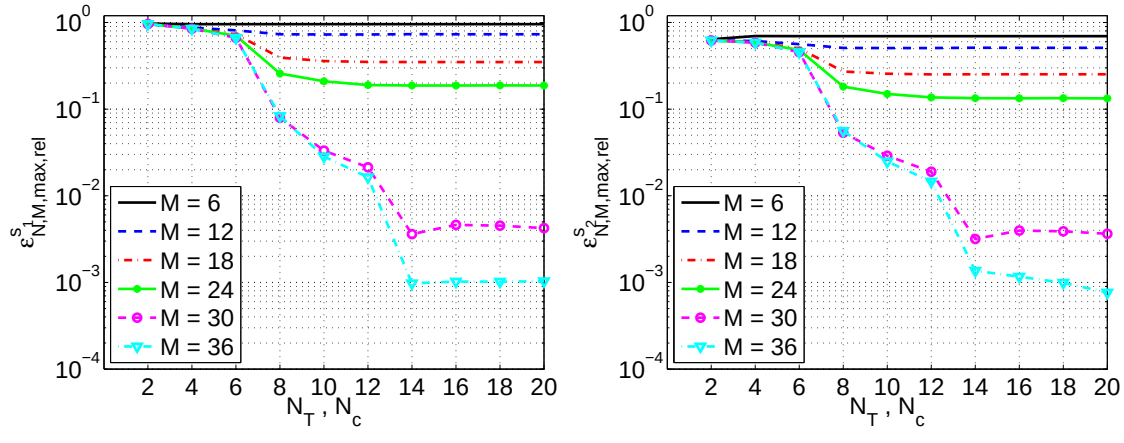


(a) (b)

Figure 9: Convergence of the reduced basis approximation: maximum relative output error.

all $k \in \mathbb{K}$ and for all $\mu \in \Xi_{\text{Test}}$. The values are normalized with respect to the computational time for the direct calculation of the truth approximation output $s_1^k(\mu)$ and $s_2^k(\mu)$ for all $k \in \mathbb{K}$. The computational savings are $O(100)$ for all values of $N = N_T = N_c$ and $M$. For an accuracy of less than 1% in the output bound ($N_T = N_c = 13$, $M = 30$) the computational savings are approximately a factor of 300.

| $N$ | $M$ | $s^k_{1/2,N,M}(\mu),\ \forall k \in \mathbb{K}$ | $s^k_{1/2}(\mu),\ \forall k \in \mathbb{K}$ |
|---|---|---|---|
| 4 | 12 | 2.22 E−03 | 1 |
| 8 | 30 | 2.74 E−03 | 1 |
| 12 | 30 | 3.42 E−03 | 1 |
| 16 | 36 | 3.96 E−03 | 1 |
| 20 | 36 | 5.12 E−03 | 1 |

Table 1: Online computational times to solve for $s^k_{1/2,N,M}(\mu)$ normalized with respect to the time to solve for $s^k_{1/2}(\mu)$ for $1 \le k \le K$.

In the one parameter case we could also obtain a very efficiently evaluable approximation of the outputs $s^k_{1,2}(\mu)$ by performing a direct interpolation of precomputed outputs at certain parameter values. We therefore compare the reduced basis output approximation with this output interpolation. To this end, we assume that we precomputed and stored the "truth" outputs $s^k_{1/2}(\mu),\ k \in \mathbb{K}$ for all $\mu \in \Xi_{\text{train}}$. Note that this step requires the same number of "truth" solves as the reduced basis offline stage. Given a new parameter value $\mu \in \mathcal{D}$, we then calculate the interpolated outputs, $s^k_{1/2,\text{int}}(\mu)$, by performing a linear interpolation at each timestep between the two precomputed solutions whose parameter values are closest to the new parameter

value. In Figures 10 and 11 we present the "truth" output, the reduced basis output, and the interpolated output as well as the errors as a function of time for the temperature and concentration output, respectively. A zoom at the time of ignition of these plots is shown in Figures 12 and 13. We note that the reduced basis output approximation performs much better than the interpolated output. This is due to the fact that the ignition times change with the parameter and the interpolation thus cannot capture the correct dynamics. We also confirm the superior behavior of the reduced basis output approximation compared to the interpolated output in Table 2, where we present the maximum relative output error $\epsilon^s_{\max,\mathrm{rel}}$ as defined previously and the maximum relative $L^2(I)$-output error $\epsilon^s_{\max,\mathrm{rel},L^2(I)}$, defined as the maximum over $\Xi_{\mathrm{Test}}$ of $\sqrt{\sum_{k=1}^K (s^k(\mu) - s^k_{N,M/\mathrm{int}}(\mu))^2}/\sqrt{\sum_{k=1}^K s^k(\mu)^2}$.

| | Reduced Basis | Interpolation |
|---|---|---|
| $\epsilon^{s_1}_{\max,\mathrm{rel}}$ | 1.39 E – 03 | 6.74 E – 01 |
| $\epsilon^{s_2}_{\max,\mathrm{rel}}$ | 1.16 E – 03 | 4.15 E – 01 |
| $\epsilon^{s_1}_{\max,\mathrm{rel},L^2(I)}$ | 2.00 E – 04 | 4.08 E – 01 |
| $\epsilon^{s_2}_{\max,\mathrm{rel},L^2(I)}$ | 5.38 E – 05 | 1.49 E – 01 |

Table 2: Comparison of maximum relative output errors for reduced basis approximation and direct interpolation of the output.

Finally, we present in Figure 14 the truth temperature output $s^k_1(\mu)$, the reduced basis output approximation $s^k_{1,N,M}(\mu)$ and the relative error $|s^k_1(\mu) - s^k_{1,N,M}(\mu)|/s_{1,\max}(\mu)$ as a function of (discrete) time for $\mu = 12.6$; here, $s_{1,\max}(\mu) = \max_{k\in\mathbb{K}} s^k_1(\mu)$. The corresponding results for the concentration output are shown in Figure 15. Note that $\mu = 12.6$ is the most

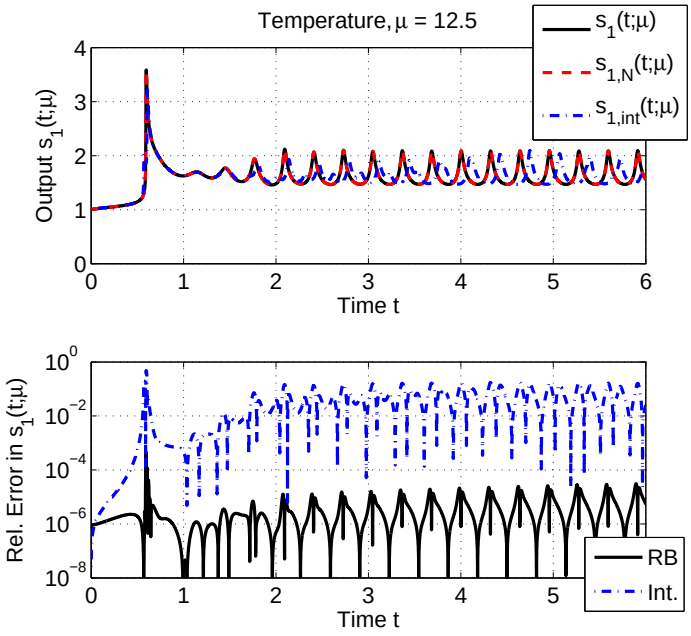


Figure 10: Comparison of reduced basis output $s_{1,N,M}(t;\mu)$ and interpolated output $s_{1,int}(t;\mu)$ for $\mu = 12.5$ and $N_T = 16$, $N_c = 16$, and $M = 36$.

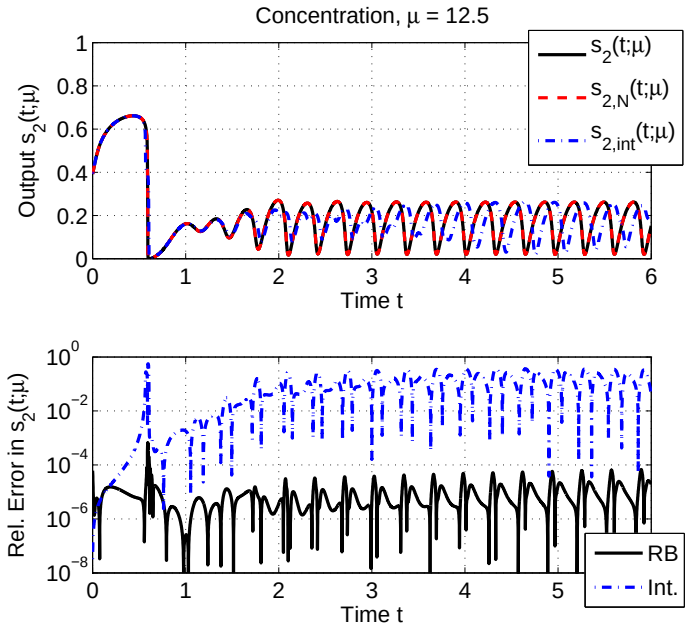


Figure 11: Comparison of reduced basis output $s_{1,N,M}(t;\mu)$ and interpolated output $s_{1,int}(t;\mu)$ for $\mu = 12.5$ and $N_T = 16$, $N_c = 16$, and $M = 36$.

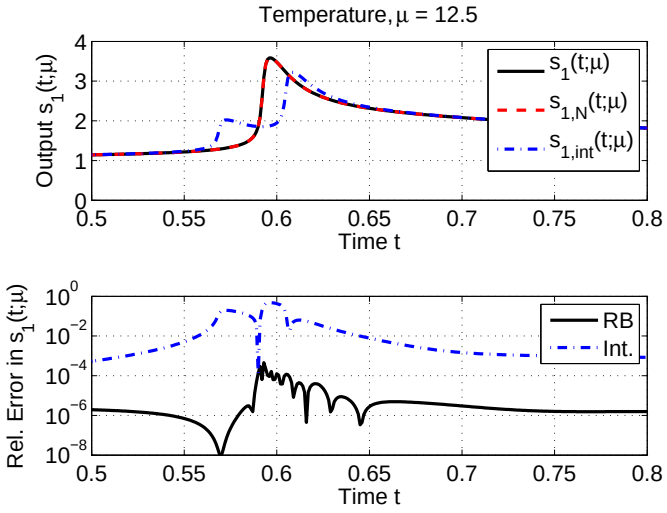


Figure 12: Comparison of reduced basis output $s_{1,N,M}(t;\mu)$ and interpolated output $s_{1,int}(t;\mu)$ for $\mu = 12.5$ and $N_T = 16$, $N_c = 16$, and $M = 36$, zoom at time of ignition.

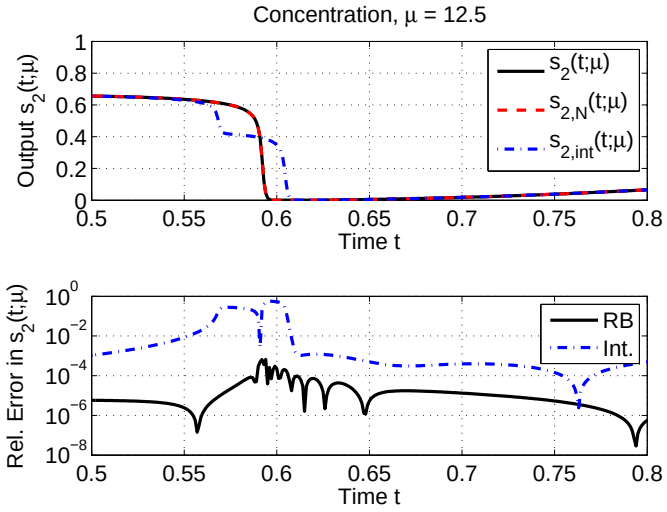


Figure 13: Comparison of reduced basis output $s_{1,N,M}(t;\mu)$ and interpolated output $s_{1,int}(t;\mu)$ for $\mu = 12.5$ and $N_T = 16$, $N_c = 16$, and $M = 36$, zoom at time of ignition.

difficult parameter value in terms of dynamic behaviour due to the highest temperature during ignition and the following mixed mode oscillation. The reduced basis approximation reproduces the the initial ignition as well as the mixed mode oscillation very well. The maximum relative error (shown on a log-scale) remains approximately on the order of $10^{-4}$ throughout the whole time interval of interest.

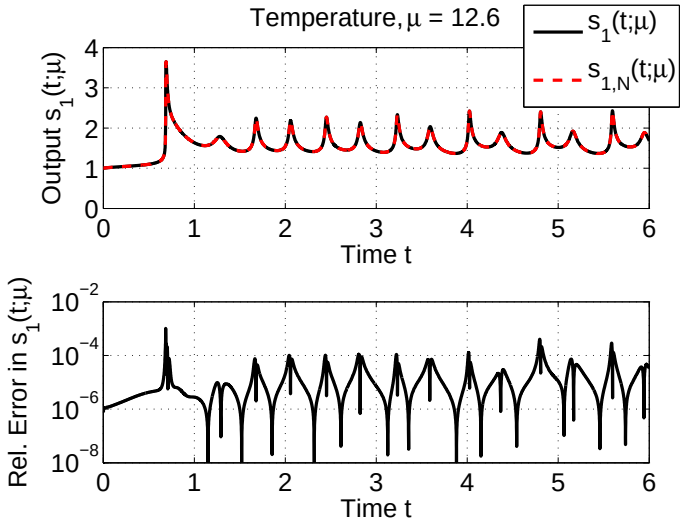


Figure 14: Output $s_1(t;\mu)$, output estimate $s_{1,N,M}(t;\mu)$, and relative output error as a function of time for $\mu = 12.6$ and $N_T = 16$, $N_c = 16$, and $M = 36$.

## 5. Conclusions

We have presented a model order reduction technique for parametrized nonlinear reaction-diffusion systems. To this end, we employed the reduced basis method, a model order reduction technique which proved very powerful for systems with simultaneous dependence on parameter and time. We

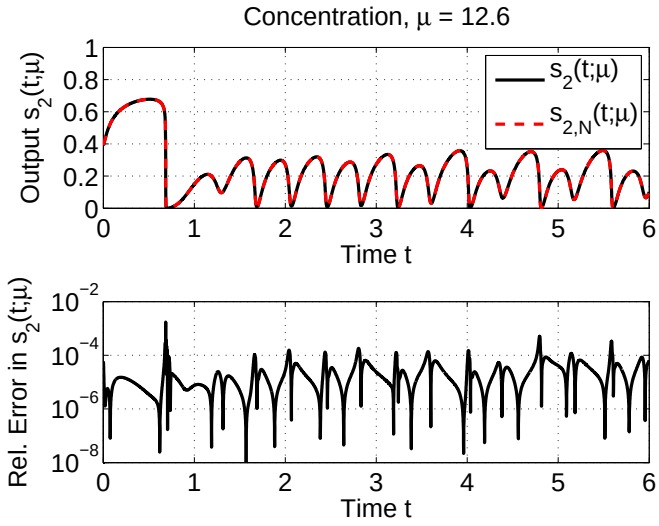


Figure 15: Output $s_2(t;\mu)$, output estimate $s_{2,N,M}(t;\mu)$, and relative output error as a function of time for $\mu = 12.6$ and $N_T = 16$, $N_c = 16$, and $M = 36$.

presented numerical results for a nonlinear reaction-diffusion system modelling the self-ignition of a coal stockpile. The reduced basis approximation converged very fast – despite the complex dynamic behavior and strong dependence on the parameter – resulting in a significant dimension reduction. The reduced basis approximation accurately captured the dynamic behavior and thus also performed clearly superior compared to a direct interpolation of the output.

Our second focus was the development of an efficient offline-online computational procedure even in the presence of strong nonlinearities. To this end, we employed the empirical interpolation method to construct an affine coefficient-function approximation of the nonlinear term. The EIM allows a complete decoupling of the offline stage — where the reduced basis spaces are generated — and the online stage — where, given a new parameter value,

we solve the reduced basis approximation and evaluate the output. The online stage depends only on $N$ and $M$ and the parametric complexity of the problem. We observed a significant $O(10^2)$ reduction in online computational time for the solution of the reduced model compared to the solution of the full model.

We thus believe that if there is a high premium on *real-time* performance or a *many-query* context — for example in the design, optimization, control, and characterization contexts — the reduced basis approach presented here can be very gainfully employed.

**Acknowledgements**

I would like to thank Professor Anthony T. Patera of MIT for many fruitful discussions and the anonymous reviewer for helpful comments. This work was supported by the Excellence Initiative of the German federal and state governments.

**Nomenclature**

| | |
|---|---|
| $()^k$ | superscript to denote timestep |
| $()^{\mathrm{e}}$ | superscript to denote "exact" (semi-discrete) quantities |
| $()_c$ | subscript to denote concentration related quantities of model problem |
| $()_N$ | subscript to denote reduced basis quantities |
| $()_T$ | subscript to denote temperature related quantities of model problem |
| $()_{N,M}$ | subscript to denote reduced basis quantities (including EIM) |

| | |
|---|---|
| $(\underline{\ })$ | vector quantities |
| $\alpha$ | thermal diffusivity |
| $\mathcal{D}$ | admissible parameter domain |
| $\Delta t$ | discrete time step size |
| $\ell$ | linear form (output functional) |
| $\gamma$ | Arrhenius number |
| $\mathbb{K}$ | set of timesteps, $\mathbb{K} \equiv \{1, \ldots, K\}$ |
| $\mu$ | parameter vector |
| $\mathcal{N}$ | finite element dimension |
| $\Omega$ | spatial domain |
| $\phi$ | finite element basis function |
| $\Theta_a^q$ | parameter dependent functions in affine decomposition of $a$ |
| $\underline{\mathrm{D}}$ | diffusion matrix |
| $\underline{A}$ | stiffness matrix |
| $\underline{B}^M$ | EIM nodal value matrix |
| $\underline{F}$ | load vector |
| $\underline{G}$ | vector containing nonlinearity |
| $\underline{M}$ | mass matrix |

$\varphi$ coefficients of EIM approximation

$\xi$ POD mode, generating function for EIM

$\Xi_{\text{train}}$ parameter train sample

$\Xi_{\text{Test}}$ parameter test sample

$\zeta$ reduced basis function

$a$ bilinear form

$a^q$ parameter independent bilinear forms in affine decomposition of $a$

$c$ normalized concentration for model problem

$f$ linear form (forcing)

$g$ nonlinear function

$g_M$ EIM interpolant of nonlinear function $g$

$I$ time interval ($\bar{I} \equiv [0, t_f]$)

$K$ number of timesteps

$M$ dimension of EIM approximation space

$m$ bilinear form

$N$ reduced basis dimension

$P$ number of parameters

$q$ EIM basis function

| | |
|---|---|
| $Q_a$ | number of terms in affine decomposition of $a$ |
| $s$ | output of interest |
| $T$ | normalized temperature for model problem |
| $t$ | time |
| $t_f$ | final time |
| $T_M^g$ | set of EIM interpolation points |
| $u$ | control input |
| $v$ | test function |
| $W_M^g$ | EIM approximation space |
| $W_N^y$ | reduced basis space |
| $x$ | spatial variable |
| $x^g$ | EIM interpolation point |
| $Y$ | approximation space |
| $y$ | field variable |
| Da | Damköhler number |

## References


J. Smoller, Shock Waves and Reaction-Diffusion Equations, Springer, 1994.

W. Marquardt, Nonlinear model reduction for optimization based control of transient chemical processes, in: Proc. 6th Int. Conf. Chem. Process Contr., volume 98 of *AIChE Symp. Ser. 326*, pp. 12–42.

S. Y. Shvartsman, C. Theodoropoulos, R. Rico-Martnez, I. G. Kevrekidis, E. S. Titi, T. J. Mountziaris, Order reduction for nonlinear dynamic models of distributed reacting systems, J. Process Contr. 10 (2000) 177 – 184.

P. Christofides, Control of nonlinear distributed process systems: Recent developments and challenges, AIChE J. 47 (2001a) 514–518.

P. Christofides, Nonlinear and Robust Control of PDE Systems, Birkhäuser, 2001b.

S. Shvartsman, I. Kevrekidis, Nonlinear model reduction for control of distributed systems: A computer-assisted study, AIChE J. 44 (1998) 1579–1595.

E. Balsa-Canto, A. Alonso, J. Banga, Reduced-order models for nonlinear distributed process systems and their application in dynamic optimization, Ind. Eng. Chem. Res. 43 (2004) 3353–3363.

K. Brooks, V. Balakotaiah, D. Luss, Effect of natural convection on spontaneous combustion of coal stockpiles, AIChE J. 34 (1988) 353–365.

F. Williams, Combustion Theory, Benjamin-Cummings, San Francisco, 1985.

N. Britton, Reaction-Diffusion Equations and Their Applications to Biology, Academic Press, 1986.

R. Aris, The Mathematical Thoery of Diffusion and Reaction in Permeable Catalysts, Vol.1, Clarendon Press, 1975a.

R. Aris, The Mathematical Thoery of Diffusion and Reaction in Permeable Catalysts, Vol.2, Clarendon Press, 1975b.

L. Sirovich, M. Kirby, Low-dimensional procedure for the characterization of human faces, J. Opt. Soc. Am. A 4 (1987) 519–524.

L. Sirovich, Turbulence and the dynamics of coherent structures, part 1: Coherent structures, Q. Appl. Math. 45 (1987) 561–571.

P. Holmes, J. Lumley, G. Berkooz, Turbulence, coherent structures, dynamical systems and symmetry, Cambridge University Press, 1996.

B. Moore, Principal component analysis in linear systems: Controllability, observability, and model reduction, IEEE T. Automat. Contr. 26 (1981) 17–32.

S. Lall, J. Marsden, S. Glavaski, Empirical model reduction of controlled nonlinear sytems, in: Proc. 14th IFAC World Congress, Beijing, China.

S. Lall, J. E. Marsden, S. Glavaski, A subspace approach to balanced truncation for model reduction of nonlinear control systems, Int. J. Robust Nonlin. 12 (2002) 519–535.

J. Hahn, T. Edgar, An improved method for nonlinear model reduction using balancing of empirical gramians, Comput. Chem. Eng. 26 (2002) 1379–1397.

K. Willcox, J. Peraire, Balanced model reduction via the proper orthogonal decomposition, AIAA J 40 (2002) 2323–2330.

C. Rowley, Model reduction for fluids using balanced proper orthogonal decomposition, Int. J. Bifurcat. Chaos 15 (2005) 997–1013.

T. Bui, M. Damodaran, K. Willcox, Proper orthogonal decomposition extensions for parametric applications in transonic aerodynamics (AIAA Paper 2003-4213), in: Proc. 15th AIAA Computational Fluid Dynamics Conference.

E. Christensen, M. Brøns, J. Sørensen, Evaluation of proper orthogonal decomposition-based decomposition techniques applied to parameter-dependent nonturbulent flows, SIAM J. Sci. Comput. 21 (2000) 1419–1434.

L. Daniel, C. S. Ong, S. C. Low, K. H. Lee, J. White, Geometrically parameterized interconnect performance models for interconnect synthesis, in: Proc. 2002 Int. Symp. Physical Design, pp. 202–207.

M. D. Gunzburger, J. S. Peterson, J. N. Shadid, Reduced-order modeling of time-dependent PDEs with multiple parameters in the boundary data, Comput. Method Appl. M. 196 (2007) 1030 – 1047.

M. Rathinam, L. Petzold, A new look at proper orthogonal decomposition, SIAM J. Numer. Anal. 41 (2003) 1893–1925.

P. Astrid, Fast reduced order modeling technique for large scale LTV systems, in: Proc. 2004 American Control Conference, volume 2, Boston, MA, pp. 762 – 767.

R. Romijn, L. Özkan, S. Weiland, J. Ludlage, W. Marquardt, A grey-box modeling approach for the reduction of nonlinear systems, J. Process Contr. 18 (2008) 906–914.

C. Prud'homme, D. Rovas, K. Veroy, Y. Maday, A. T. Patera, G. Turinici, Reliable real-time solution of parametrized partial differential equations: Reduced-basis output bound methods, J. Fluids Eng. 124 (2002) 70–80.

G. Rozza, D. Huynh, A. Patera, Reduced basis approximation and a posteriori error estimation of affinely parametrized elliptic coercive partial differential equations, Arch. Comput. Method E. 15 (2008) 229–275.

M. Grepl, A. Patera, A posteriori error bounds for reduced-basis approximations of parametrized parabolic partial differential equations, ESAIM: Math. Model. Num. 39 (2005) 157–181.

D. Rovas, L. Machiels, Y. Maday, Reduced basis output bounds methods for parabolic problems, IMA J. Appl. Math. (2005).

B. Haasdonk, M. Ohlberger, Reduced basis method for finite volume approximations of parametrized linear evolution equations, ESAIM: Math. Model. Num. 42 (2008) 277–302.

K. Veroy, A. T. Patera, Certified real-time solution of the parametrized steady incompressible Navier-Stokes equations; Rigorous reduced-basis *a posteriori* error bounds, Int. J. Numer. Meth. Fl. 47 (2005) 773–788.

M. Grepl, Y. Maday, N. Nguyen, A. Patera, Efficient reduced-basis treatment of nonaffine and nonlinear partial differential equations, ESAIM: Math. Model. Num. 41 (2007) 575–605.

N. C. Nguyen, J. Peraire, An efficient reduced-order modeling approach for non-linear parametrized partial differential eq uations, Int. J. Num. Meth. Eng. 76 (2008) 27–55.

D. Knezevic, N. Nguyen, A. Patera, Reduced basis approximation and a posteriori error estimation for the parametrized unsteady Boussinesq equations, Math. Mod. Meth. Appl. S. 21 (2011) 1415–1442.

M. A. Grepl, Reduced-Basis Approximations and A Posteriori Error Estimation for Parabolic Partial Differential Equations, Ph.D. thesis, Massachusetts Institute of Technology, 2005.

S. Adjerid, J. E. Flaherty, A moving finite element method with error estimation and refinement for one-dimensional time dependent partial differential equations, SIAM J. Numer. Anal. 23 (1986) pp. 778–796.

A. Kapila, Asymptotic treatment of chemically reacting systems, Elsevier Science Pub. Co. Inc., New York, NY, 1983.

M. Barrault, N. C. Nguyen, Y. Maday, A. T. Patera, An "empirical interpolation" method: Application to efficient reduced-basis discretization of partial differential equations, C. R. Acad. Sci. Paris, Ser. I. 339 (2004) 667–672.

S. Chaturantabut, D. C. Sorensen, Nonlinear model reduction via discrete empirical interpolation, SIAM J. Sci. Comp. 32 (2010) 2737–2764.

O. Lass, S. Volkwein, Pod galerkin schemes for nonlinear elliptic-parabolic systems, 2011. Submitted.

M. Grepl, Certified reduced basis methods for nonaffine linear time-varying and nonlinear parabolic partial differential equations, Math. Mod. Meth. Appl. S. (2012). To appear.

Y. Maday, N. Nguyen, A. Patera, S. Pau, A general multipurpose interpolation procedure: The magic points, Commun. Pur. Aappl. Anal. 8 (2009) 383–404.

J. Eftang, M. Grepl, A. Patera, A posteriori error bounds for the empirical interpolation method, C. R. Acad. Sci. Paris, Ser. I 348 (2010) 575–579.

K. Veroy, C. Prud'homme, A. T. Patera, Reduced-basis approximation of the viscous Burgers equation: Rigorous *a posteriori* error bounds, C. R. Acad. Sci. Paris, Ser. I 337 (2003) 619–624.

D. Schmal, J. Duyzer, J. van Heuven, A model for the spontaneous heating of coal, Fuel 64 (1985) 963–972.

K. Brooks, S. Bradshaw, D. Glasser, Spontaneous combustion of coal stockpiles - an unusual chemical reaction engineering problem, Chem. Eng. Sci. 43 (1988) 2139 – 2145.

K. Brooks, D. Glasser, A simplified model of spontaneous combustion in coal stockpiles, Fuel 65 (1986) 1035 – 1041.

A. Salinger, R. Aris, J. Derby, Modeling the spontaneous ignition of coal stockpiles, AIChE Journal 40 (1994) 991–1004.